Spectroscopic factors of magic and semimagic nuclei within the self-consistent theory of finite Fermi systems.

N. V. Gnezdilov and E. E. Saperstein
Kurchatov Institute, 123182 Moscow, Russia

S. V. Tolokonnikov
Kurchatov Institute, 123182 Moscow, Russia and
Moscow Institute of Physics and Technology, 141700 Dolgoprudny, Russia.

arXiv:1407.3357v2 [nucl-th] 20 Sep 2014

A scheme is presented to find single-particle spectroscopic factors (SF) of magic and semimagic nuclei within the self-consistent theory of finite Fermi systems (TFFS). In addition to the energy dependence of the mass operator Σ induced by the surface-phonon coupling effects which are commonly considered in this problem, the in-volume energy dependence of the operator Σ inherent in the self-consistent TFFS is also taken into account. This dependence arises due to the effect of high-lying particle-hole excitations and persists in nuclear matter. The self-consistent basis of the energy density functional method by Fayans *et al.* is used. Both the surface and in-volume contributions to the SFs turned out to be of comparable magnitude. The results for magic ^{40,48}Ca and ^{208}Pb nuclei and semimagic lead isotopes are presented.

PACS numbers: 21.60.Jz, 21.10.Jx, 24.50.+g.

I. INTRODUCTION

A single-particle spectroscopic factor (SF) is an important characteristic of the single-particle state [1]. In the many-body approaches to nuclear theory [2, 3] it is expressed in terms of the so-called Z-factor, the residue of the single-particle Green function $G(\mathbf{r_1}, \mathbf{r_2}; \varepsilon)$,

$$Z(\mathbf{r}_1, \mathbf{r}_2) = \left(1 - \left(\frac{\partial \Sigma(\mathbf{r_1}, \mathbf{r_2}; \varepsilon)}{\partial \varepsilon}\right)_{\varepsilon=\varepsilon_\lambda}\right)^{-1}, \quad (1)$$

where ε_λ is the single-particle energy of the state under consideration and $\Sigma(\mathbf{r_1}, \mathbf{r_2}; \varepsilon)$ is the mass operator, $G = G_0 + G_0 \Sigma G$. Here we use the notation of theory of finite Fermi systems (TFFS) [4].

Usually the energy dependence of the mass operator is supposed to be the result of the coupling of particles with the surface vibrations ("phonons") [3, 5, 6]. In the self-consistent TFFS [7], the in-volume energy dependence of the mass operator does also exist. It arises due to the contribution to the operator Σ of high-lying collective excitations, the giant resonances, and non-collective particle-hole excitations as well. As it is shown below, the contribution of this term to the Z-factor (1) is comparable to that from the phonon coupling (PC) effects. The in-volume term depends weakly on the nucleus under consideration and the single-particle state λ, whereas the PC one fluctuates strongly.

In this work, we deal with magic nuclei or with non-superfluid components of semi-magic nuclei. In this case, simple formulas for PC corrections to nuclear characteristics in systems without pairing [8–10] can be used. In practice, we found proton and neutron SFs in magic ^{40,48}Ca and ^{208}Pb nuclei and proton ones in semimagic lead isotopes. Calculations are carried out with the use of the self-consistent basis generated by the energy density functional (EDF) by Fayans *et al.* [11] with the set of parameters DF3-a [12].

II. BRIEF FORMALISM

The self-consistent TFFS approach [7, 13] was formulated for nuclei without pairing in terms of the quasiparticle Lagrangian L_q, $L_q = \int d\mathbf{r} \mathcal{L}_q(\mathbf{r})$, which is constructed to generate the quasiparticle mass operator Σ_q. By definition [4, 7], the latter coincides with the exact mass operator Σ at the Fermi surface. In the mixed coordinate-momentum representation, $\Sigma_q(\mathbf{r}, k^2; \varepsilon)$ depends linearly on the momentum squared k^2 and on the energy ε as well,

$$\Sigma_q(\mathbf{r}, k^2; \varepsilon) = \Sigma_0(\mathbf{r}) + \frac{1}{2m\varepsilon_{\rm F}^0}\hat{\mathbf{k}}\Sigma_1(\mathbf{r})\hat{\mathbf{k}} + \Sigma_2(\mathbf{r})\frac{\varepsilon}{\varepsilon_{\rm F}^0}, \quad (2)$$

where $\varepsilon_{\rm F}^0 = k_{\rm F}^2/2m$ is the Fermi energy of nuclear matter. In magic nuclei which are non-superfluid, the Lagrangian density $\mathcal{L}_q$ depends on three sorts of densities $\nu_i(\mathbf{r}), i = 0, 1, 2$. The first two are analogs of the SHF densities $\rho(\mathbf{r}), \tau(\mathbf{r})$, whereas the density $\nu_2(\mathbf{r})$ is a new ingredient of the self-consistent theory being the single-particle energy density. In the explicit form, these densities are as follows:

$$\nu_0(\mathbf{r}) = \sum n_\lambda \psi_\lambda^*(\mathbf{r})\psi_\lambda(\mathbf{r}), \quad (3)$$

$$\nu_1(\mathbf{r}) = \frac{1}{2m\varepsilon_{\rm F}^0}\sum n_\lambda \nabla\psi_\lambda^*(\mathbf{r})\nabla\psi_\lambda(\mathbf{r}), \quad (4)$$

$$\nu_2(\mathbf{r}) = \frac{1}{\varepsilon_{\rm F}^0}\sum n_\lambda \varepsilon_\lambda \psi_\lambda^*(\mathbf{r})\psi_\lambda(\mathbf{r}), \quad (5)$$

where ε_λ and n_λ are the quasiparticle energies and occupation numbers. The quasiparticle wave functions in Eqs. (3) – (5) are normalized with the weight,

$$\int d\mathbf{r}\,\psi^*_\lambda(\mathbf{r})\,\psi_{\lambda'}(\mathbf{r})\,\left(1-\Sigma_2(\mathbf{r})/\varepsilon^0_{\rm F}\right)=\delta_{\lambda\lambda'}. \qquad (6)$$

The usual density $\rho(\mathbf{r})$ normalized to the total particle number is

$$\rho(\mathbf{r})=\left(1-\Sigma_2(\mathbf{r})/\varepsilon^0_{\rm F}\right)\nu_0(\mathbf{r}). \qquad (7)$$

The Z-factor (1) we are interested is determined with the energy derivative

$$\frac{\partial\Sigma_q(\mathbf{r})}{\partial\varepsilon}=\Sigma_2(\mathbf{r})/\varepsilon^0_{\rm F}. \qquad (8)$$

In its turn, the Σ_2 operator is

$$\Sigma_2(\mathbf{r})=\frac{\delta L_q}{\delta\nu_2}. \qquad (9)$$

The simplest form of the corresponding term of the quasiparticle Lagrangian was proposed in [7, 13] yielding

$$\Sigma_2(\mathbf{r})=C_0\lambda_{02}\nu_0(\mathbf{r}), \qquad (10)$$

where $C_0=(dn/d\varepsilon^0_{\rm F})^{-1}=\pi^2/mp^0_{\rm F}$ is the usual TFFS normalization factor, the inverse density of states at the Fermi surface. The dimensionless parameter $\lambda_{02}=-0.25$ is used below, which is found in [7] for the best description of the single particle spectra of magic nuclei. It corresponds to the value $Z_0=0.8$ of the Z-factor in nuclear matter. This value agrees with the one found in [14, 15] from the dispersion relation for the quantity $\partial\Sigma/\partial\varepsilon$ in nuclear matter.

With the use of Eqs. (1), (7), (8) and (10), the Z-factor can be expressed directly in terms of the usual density,

$$Z_0(\mathbf{r})=\frac{2}{1+\sqrt{1-4C_0\lambda_{02}\rho(\mathbf{r})/\varepsilon^0_{\rm F}}}. \qquad (11)$$

The self-consistent evaluation of the PC corrections to the mass operator in magic nuclei was studied in [9] with the analysis of single-particle energies. In this work we use the same approach for spectroscopic factors.

In accordance with Eq. (1), the PC contribution to the single-particle Z-factor is

$$Z^{\rm PC}=\left(1-\left.\frac{\partial\delta\Sigma^{\rm PC}}{\partial\varepsilon}\right|_{\varepsilon=\varepsilon_\lambda}\right)^{-1}, \qquad (12)$$

where $\delta\Sigma^{\rm PC}$ is the PC correction to the quasiparticle mass operator Σ_q. Here we deal with the perturbation theory in $\delta\Sigma$ operator with respect to the quasiparticle Hamiltonian H_0. As well as in [8–10], we use the so-called g_L^2-approximation which is, as a rule, applicable to magic nuclei. Here g_L is the L-phonon creation amplitude. Actually, g_L^2-correction to the mass operator contains two terms [7],

$$\delta\Sigma^{\rm PC}=\delta\Sigma^{\rm pole}+\delta\Sigma^{\rm tad}, \qquad (13)$$

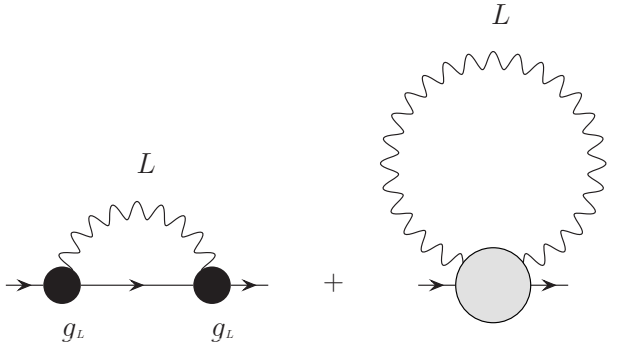

FIG. 1: PC corrections to the mass operator. The gray blob denotes the "tadpole" term.

which are shown in Fig. 1.

In obvious symbolic notation, the pole diagram corresponds to $\delta\Sigma^{\rm pole}=(g_L,DGg_L)$ where $D_L(\omega)$ is the phonon D-function. Explicitly one obtains

$$\delta\Sigma^{\rm pole}_{\lambda\lambda}(\epsilon)\;=\;\sum_{\lambda_1\,M}|\langle\lambda_1|g_{LM}|\lambda\rangle|^2 \times\left(\frac{n_{\lambda_1}}{\varepsilon+\omega_L-\varepsilon_{\lambda_1}}+\frac{1-n_{\lambda_1}}{\varepsilon-\omega_L-\varepsilon_{\lambda_1}}\right), \qquad (14)$$

where ω_L is the excitation energy of the L-phonon and $n_\lambda=(0,1)$ stands for occupation numbers.

The vertex g_L in Eq. (14) reads [4]

$$g_L(\omega)=\mathcal{F}A(\omega)g_L(\omega), \qquad (15)$$

where $A(\omega)=\int G\left(\varepsilon+\omega/2\right)G\left(\varepsilon-\omega/2\right)d\varepsilon/(2\pi i)$ is the particle-hole propagator, $G(\varepsilon)$ being the single-particle Green function.

As for the second, tadpole, term in Fig. 1, it is equal to

$$\delta\Sigma^{\rm tad}=\int\frac{d\omega}{2\pi i}\delta_L g_L D_L(\omega), \qquad (16)$$

where $\delta_L g_L$ can be found [7] by variation of Eq. (15) in the field of the L-phonon. We do not focus on the term $\delta\Sigma^{\rm tad}$ because it does not depend on the energy ε. Hence, it does not contribute to $Z^{\rm PC}$. Vertices g_L and the tadpole term are considered in more detail in [9].

Thus, the energy derivative of the mass operator, which enters into (12), is equal to

$$\left.\frac{\partial\delta\Sigma^{\rm pole}_{\lambda\lambda}(\varepsilon)}{\partial\varepsilon}\right|_{\varepsilon=\varepsilon_\lambda}\;=\;-\sum_{\lambda'\,M}|<\lambda'|g_{LM}|\lambda>|^2 \times\left[\frac{n_{\lambda'}}{(\varepsilon_\lambda+\omega_L-\varepsilon_{\lambda'})^2}\;+\;\frac{1-n_{\lambda'}}{(\varepsilon_\lambda-\omega_L-\varepsilon_{\lambda'})^2}\right]. \qquad (17)$$

With the use of Eqs. (1) and (12), one obtains the total single-particle Z-factor allowing for PC effects,

$$Z_\lambda=Z_{0\lambda}\left(1-Z_{0\lambda}\,\frac{\partial}{\partial\varepsilon}\delta\Sigma^{\rm pole}_{\lambda\lambda}\right|_{\varepsilon=\varepsilon_\lambda}\Bigg)^{-1}, \qquad (18)$$

where $Z_{0\lambda} =< \lambda|Z_0(\mathbf{r})|\lambda >$.

The typical value of the denominators in the sum (17) is $\sim \varepsilon_{\rm F} A^{-1/3}$. However, there are some cases when one of them is close to zero. This happens often in semimagic nuclei where the excitation energy of the first 2^+-state is $\omega_2 \sim 1$ MeV. In this case, the single-particle states λ, λ' which have the same parity and belong to the same shell can possess close energies, so that one gets $|\varepsilon_\lambda - \varepsilon_{\lambda'}| \cong \omega_L$. As a result, the simple perturbation theory used in (17) should be modified with separating the couple of "dangerous" states (λ_0, λ_0'). Let us, e. g., have $\varepsilon_{\lambda_0} \cong \varepsilon_{\lambda_0'} - \omega_L$. Then, for $\lambda = \lambda_0$, we extract the term with $\lambda' = \lambda_0'$ in the sum (17). Let us denote the corresponding value of the phonon Z-factor as Z'. The next step is the exact solution of the two-level problem of mixing the states $|\lambda_0\rangle$ and $|\lambda_0' + 2_1^+\rangle$. However, there are cases of almost exact generation of these states with a trivial solution of this problem. Namely, both mixing coefficients are equal to $\sqrt{2}$. In this case, the phonon Z-factor is equal to

$$Z_{\lambda_0}^{\rm PC} = \frac{1}{\sqrt{2}}\, Z'_{\lambda_0}. \qquad (19)$$

All the above formulas are written for magic nuclei in which the pairing does not exist. They are valid also for the normal component of a semimagic nucleus, with a sole exception. As far as the second component is superfluid, the RPA-like Eq. (15) should be replaced with the QRPA-like TFFS equation for nuclei with pairing [4]. In practice, we used the scheme developed for superfluid nuclei in [16].

III. CALCULATION RESULTS

Before we start to discuss the calculation results for SFs, a comment on the "experimental" data should be made. We took the word "experimental" in quotes as this term could be used for the corresponding data, say, in the database [17], rather conventionally. Indeed, "a lot of theory" is used to extract SFs from the experimental cross sections. Typically, SFs are found from the analysis of (d,p) or (d,n) reactions within the Distorted Wave Born Approximation (DWBA). Such a procedure was convincingly criticized in Ref. [18] titled "Non-observability of Spectroscopic Factors". Arguments are given that the ansatz for the energy dependence of the optical potential used in the DWBA calculation affects the SF values more than the measured cross-sections. In such a situation, it is concluded in [18] that it is more reasonable to put attention to a tendency in variance of SF values found in a series of experiments, e. g. for a chain of isotopes, than for their absolute values. The reaction $(e,e'p)$ could be also used for extracting SFs, being simpler for the analysis than deuteron induced reactions. However, as the analysis in Ref. [19] shows, even in this most simple reaction there are doubts in a possibility to extract the occupation numbers consistently. Below, we will omit the quotation marks in the word experimental keeping them in mind.

TABLE I: Spectroscopic factors in ^{208}Pb. Experimental data are taken from [17] and from [22], marked with ^{a}.

λ	ε_λ	Z_0	$Z^{\rm PC}$	$Z_{\rm tot}$	$S_{\rm exp}$
$3d^n_{3/2}$	-0.709	0.852	0.879	0.763	0.74
$4s^n_{1/2}$	-1.080	0.848	0.895	0.771	0.8
$2g^n_{7/2}$	-1.091	0.849	0.886	0.765	0.9
$3d^n_{5/2}$	-1.599	0.848	0.873	0.755	0.85
$1j^n_{15/2}$	-2.167	0.830	0.618	0.549	0.53
$1i^n_{11/2}$	-2.511	0.838	0.945	0.799	0.9
$2g^n_{9/2}$	-3.674	0.833	0.882	0.749	0.8
$3p^{-n}_{1/2}$	-7.506	0.834	0.926	0.782	1.1, 0.9^a
$3p^{-n}_{3/2}$	-8.363	0.822	0.913	0.762	0.96, 0.88^a
$2f^{-n}_{5/2}$	-8.430	0.828	0.923	0.775	0.88, 0.6^a
$1i^{-n}_{13/2}$	-9.411	0.822	0.902	0.755	0.49, 0.91^a
$2f^{-n}_{7/2}$	-10.708	0.816	0.567	0.503	0.55, 0.95^a
$1h^{-n}_{9/2}$	-11.009	0.820	0.892	0.746	0.56, 0.98^a
$3p^p_{3/2}$	-0.249	0.853	0.690	0.617	1.03
$2f^p_{5/2}$	-0.964	0.850	0.812	0.710	1.15
$1i^p_{13/2}$	-2.082	0.836	0.741	0.646	0.88
$2f^p_{7/2}$	-3.007	0.842	0.859	0.740	1.18
$1h^p_{9/2}$	-4.232	0.837	0.958	0.807	0.95
$3s^{-p}_{1/2}$	-7.611	0.838	0.929	0.787	0.85^a
$2d^{-p}_{3/2}$	-8.283	0.827	0.937	0.783	0.9^a
$1h^{-p}_{11/2}$	-8.810	0.832	0.931	0.784	0.88^a
$2d^{-p}_{5/2}$	-9.782	0.826	0.711	0.618	0.65^a
$1g^{-p}_{7/2}$	-11.735	0.820	0.423	0.387	0.52^a

It should be stressed that our calculations do not contain any new parameters. The set DF3-a parameters [12] of the Fayans functional proved to be rather successful in describing various nuclear characteristics including nuclear charge radii [20], the excitation energies and $BE2$ values for 2_1^+ states in lead and tin isotopes [16], the quadrupole moments of odd nuclei [21], PC corrections to magnetic moments [8, 10], and single-particle levels of magic nuclei [9]. As to the parameter λ_{02} governing the value of Z_0 in nuclear matter, it was found in [7] from the analysis of single-particle spectra in magic nuclei. The value was confirmed [14, 15] with the analysis of the dispersion relation for the quantity $\partial\Sigma/\partial\varepsilon$ in nuclear matter. In its turn, the latter was resolved in terms of the known Landau–Migdal parameters.

Let us begin the analysis from the double magic ^{208}Pb, ^{40}Ca and ^{48}Ca nuclei, tables 1–3, with the greatest amount of the experimental data on SFs. We took the data mainly from the database [17]. The latter typically contains several values for the state and the nucleus under consideration taken from different original works which sometimes are significantly different, in agreement with [18]. As a rule, we chose the freshest one, just to have some formal how-to-do recipe. In several cases we used

TABLE II: Spectroscopic factors in ^{40}Ca. Experimental data are taken from [17].

λ	ε_λ	Z_0	$Z^{\rm PC}$	$Z_{\rm tot}$	$S_{\rm exp}$
$1f^{n}_{5/2}$	-2.124	0.910	0.947	0.866	0.9
$2p^{n}_{1/2}$	-3.729	0.917	0.934	0.861	0.7
$2p^{n}_{3/2}$	-5.609	0.905	0.916	0.836	0.91
$1f^{n}_{7/2}$	-9.593	0.893	0.947	0.850	0.77
$1d^{-n}_{3/2}$	-14.257	0.871	0.965	0.844	0.94
$2s^{-n}_{1/2}$	-15.780	0.875	0.930	0.821	0.82
$1d^{-n}_{5/2}$	-19.985	0.868	0.969	0.844	0.9
$1f^{p}_{5/2}$	4.359	0.921	0.963	0.890	0.33
$2p^{p}_{1/2}$	2.456	0.935	0.950	0.891	0.75
$2p^{p}_{3/2}$	0.936	0.916	0.966	0.887	0.94
$1f^{p}_{7/2}$	-2.678	0.896	0.960	0.864	1.12
$1d^{-p}_{3/2}$	-7.264	0.874	0.966	0.848	0.93
$2s^{-p}_{1/2}$	-8.663	0.878	0.931	0.825	0.87
$1d^{-p}_{5/2}$	-12.856	0.870	0.969	0.846	0.83

TABLE III: Spectroscopic factors in ^{48}Ca. Experimental data are taken from [17].

λ	ε_λ	Z_0	$Z^{\rm PC}$	$Z_{\rm tot}$	$S_{\rm exp}$
$1g^{n}_{9/2}$	0.836	0.915	0.796	0.741	0.47
$2p^{n}_{1/2}$	-3.890	0.880	0.773	0.699	1.03
$2p^{n}_{3/2}$	-5.784	0.854	0.939	0.809	0.97
$1f^{-n}_{7/2}$	-9.488	0.870	0.965	0.844	0.85
$2p^{p}_{1/2}$	-3.549	0.883	0.648	0.596	0.88
$1f^{p}_{5/2}$	-4.048	0.890	0.873	0.788	-
$2p^{p}_{3/2}$	-4.731	0.880	0.604	0.558	0.54
$1f^{p}_{7/2}$	-9.909	0.865	0.899	0.789	0.91
$2s^{-p}_{1/2}$	-15.098	0.853	0.915	0.791	0.92
$1d^{-p}_{3/2}$	-16.172	0.858	0.917	0.796	1.22

TABLE IV: Spectroscopic factors of proton states in semimagic isotopes ^{204,206}Pb. Experimental data are taken from [17]. * marks the case when the $Z^{\rm PC}$ was found from Eq. (19).

A	λ	ε_λ	Z_0	$Z^{\rm PC}$	$Z_{\rm tot}$	$S_{\rm exp}$
206	$1i^{p}_{13/2}$	-1.666	0.836	0.821	0.707	0.90
	$2f^{p}_{7/2}$	-2.513	0.842	0.817	0.708	0.82
	$1h^{p}_{9/2}$	-3.818	0.838	0.880	0.752	0.90
	$3s^{-p}_{3/2}$	-7.178	0.839	0.926	0.786	0.64
	$2d^{-p}_{3/2}$	-8.283	0.827	0.327	0.306	0.49
	$1h^{-p}_{11/2}$	-8.416	0.832	0.859	0.732	0.61
204	$1i^{p}_{13/2}$	-1.210	0.836	0.683	0.602	0.82
	$2f^{p}_{7/2}$	-2.010	0.843	0.702	0.620	0.53
	$1h^{p}_{9/2}$	-3.356	0.838	0.773	0.673	0.90
	$3s^{-p}_{3/2}$	-6.717	0.839	0.866	0.743	0.7
	$2d^{-p}_{3/2}$ *	-7.505	0.827	0.575	0.513	0.46
	$1h^{-p}_{11/2}$	-7.977	0.833	0.739	0.644	0.68

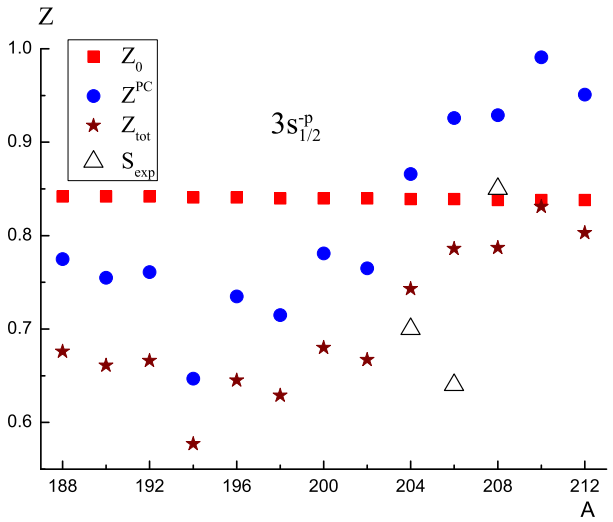

FIG. 2: (Color online) Spectroscopic factors of the proton hole $3s^{-p}_{1/2}$ state in Pb isotopes.

also the experimental SFs from [22] where some original experimental works were used in addition to [17]. Each table contains three values for the Z-factor which are the theoretical predictions for the SF. Z_0 takes into account only in-volume energy dependence of the quasiparticle mass operator (2) within the self-consistent TFFS. $Z^{\rm PC}$ is the SF originating only from the PC contributions. At last, $Z_{\rm tot}$ is the total SF which takes into account both effects via Eq. (18).

As it was discussed above, the experimental values of SFs have large uncertainties. This is particularly evident in several cases with $S_{\rm exp} \geq 1$. This permits to suspect that in many other cases the normalization of SFs could also be doubtful. Tables 1–3 contain four such "bad" cases for ^{208}Pb, one for ^{40}Ca, and two for ^{48}Ca. In addition to direct experimental inaccuracies, these uncertainties appear because of the way to extract SFs from the data on the one-nucleon transfer reactions using the DWBA. Dropping at a time the principle objections [18] against the method itself, there is a lot of practical uncertainties in the procedure. In particular, the parameters of optical potentials used in the DWBA calculations are not known sufficiently well, especially the spin-orbit ones.

To understand which of three theoretical values for the Z-factor should be compared to the experimental SF, let us for a moment forget about principle problems with the DWBA approach and imagine that there exists a perfect theory for describing reactions (d,p) and (d,n). At small energy of the deuteron projectile and, correspondingly, small momentum transfer $q \ll k_{\rm F}$, the wave functions of the outgoing nucleon and the one absorbed with the

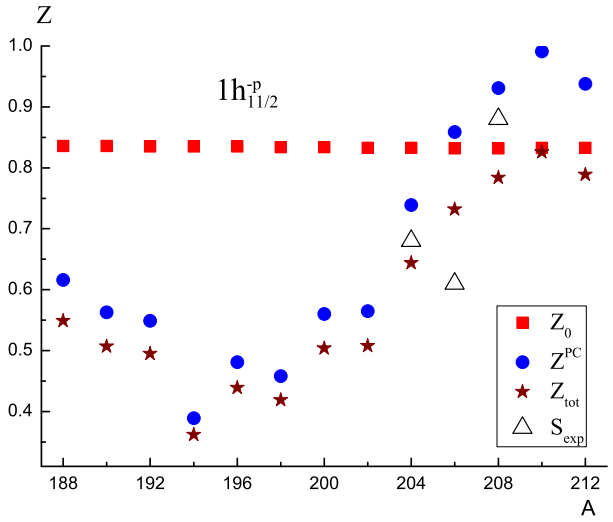

FIG. 3: (Color online) Spectroscopic factors of the proton hole $1h^{-p}_{11/2}$ state in Pb isotopes.

target nucleus "have time" to adapt to the mean field of the nucleus which, according to TFFS [4], involves the factor Z_0: $U(\mathbf{r}) = Z_0(\mathbf{r})\Sigma_q(\mathbf{r})$. Therefore the SF extracted from such a reaction includes only the spread of the single-particle state under consideration over nearlying many-particle configurations, those with PC contributions being the most important. In this case, the value of $Z^{\rm PC}_\lambda$ should be compared to $S_{\rm exp}$. Another situation takes place in the case of large values of the deuteron energy and momentum transfer $q \gg k_{\rm F}$. In this limit, the field created by the projectile feels "bare" nucleons. The weight of a bare nucleon in the state under consideration is equal to $Z_{0\lambda}$. As a result, the experimental SF should be compared with the total Z-factor $Z^{\rm tot}_\lambda$.

For relevant choice between $Z^{\rm PC}$ and $Z_{\rm tot}$ values, it is necessary to make a detailed analysis of the experimental details and the theoretical method used for description of the reaction data. It is practically impossible as far as the most of the experiments presented in [17] are rather updated. In absence of such analysis, we are forced to use some intermediate value between the phonon and total SFs to compare with $S_{\rm exp}$. It should be mentioned also that the data on SF in [17] do not contain as a rule the experimental bars. This stresses that the authors of the original works consider the accuracy of extracting SF as rather poor. In such a situation, it is hardly reasonable to make a detailed comparison with the data. If we exclude from the analysis four cases with $S_{\rm exp} \geq 1$, a rough analysis shows that the experimental value is, as a rule, in the interval between $Z_{\rm tot}$ and $Z^{\rm PC}$. The cases of preference of each limit value are divided approximately in half. As in [8–10], the PC Z-factor in ^{208}Pb was found by taking into account nine phonons: 3^-, two phonons 5^- and six phonons of positive parity, $2^+_{1,2}$, $4^+_{1,2}$, and $6^+_{1,2}$. Just as in calculations of the PC contributions to the single-particle spectra [9], the contribution of the 3^- phonon as a rule dominates. However, sometimes the total contribution of other phonons is comparable to the one of 3^-. Let us recall that $Z^{\rm PC}$ is found in the g^2_L approximation which is valid provided we get $1 - Z^{\rm PC} \ll 1$. This approximation evidently fails for the state $1g^{-p}_{7/2}$, see the last line in Table 1. This explains why the corresponding values $Z^{\rm PC}$ and $Z_{\rm tot}$ are too small to explain the datum. Next correction in g^2_L should make $Z^{\rm PC}$ greater, closer to $S_{\rm exp}$. Another situation takes place for the state $1i^p_{13/2}$. In this case, the g^2_L approximation is valid and we believe in the theoretical result. We suspect that, just as for its neighbors in the table, it is worth to recall the quotation marks in the word "experimental".

In the ^{40}Ca nucleus, Table 2, the value of $Z_{\rm tot}$ agrees as a rule better with the data. There is only one third of cases where the $Z^{\rm PC}$ value happens to be better. In this nucleus the single 3^- phonon ($\omega_{3-} = 3.335$ MeV, $\omega^{\rm exp}_{3-} = 3.737$ MeV) contributes to PC effects. Although it is strongly collective [$BE3 = 22.9$ WU, $BE3^{\rm exp} = 27(4)$ WU], $Z^{\rm PC}$ values turn out to be close to unity, as all energy denominators in (17) are very large because of the large values of both proton and neutron magic gaps. In the ^{48}Ca nucleus, just as ^{208}Pb, the cases of the preferred $Z^{\rm PC}$ and $Z_{\rm tot}$ values are approximately bisected. In this nucleus, two phonons, 3^- ($\omega_{3-} = 4.924$ MeV, $\omega^{\rm exp}_{3-} = 4.507$ MeV) and 2^+ ($\omega_{2+} = E = 3.576$ MeV, $\omega^{\rm exp}_{2+} = 3.832$ MeV), contribute to $Z^{\rm PC}$ approximately equally. In this nucleus, the difference $(1 - Z^{\rm PC})$ is, as a rule, bigger than in ^{40}Ca as now the neutron energy denominators of Eq. (17) are much smaller. In Ca isotopes, there are two cases, $1f^p_{5/2}$-state in ^{40}Ca and $1g^n_{9/2}$-state in ^{48}Ca, where a strong disagreement with the data is observed. In both cases, just as for the $1i^p_{13/2}$-state in ^{208}Pb, we believe that our predictions are more reliable.

In semimagic nuclei, the situation is essentially different due to the presence of the low-lying 2^+ phonon which is strongly collective and dominates in all PC effects. As a result, the difference of $Z^{\rm PC}$ from unity is, as a rule, bigger than in magic nuclei. It makes sometimes questionable application of the perturbation theory used above for describing the PC effects. We consider the proton SFs in the chain of the even semimagic lead isotopes $^{188-212}$Pb. Unfortunately, the data on SFs in these nuclei are scarce. Therefore Table 4 contains two nuclei only, ^{204}Pb and ^{206}Pb, for which the database [17] contains some data on SFs. Predictions for all the chain are displayed in figs. 2 and 3 for the states $3s^{-p}_{1/2}$ and $1h^{-p}_{11/2}$, respectively.. They are chosen because, firstly, their experimental SFs are known in the nuclei listed above and, secondly, there is a hope for measurement of their SFs in other nuclei. Indeed, the state $3s^{-p}_{1/2}$ there is right at the Fermi surface and therefore is readily populated in one-nucleon transfer reactions. As to the $1h^{-p}_{11/2}$ state, it has a high value of the angular momentum which makes the cross section of its excitation larger. It is worth to note that there are three cases on fig. 3 with $Z^{\rm PC} \preceq 0.5$, where the g^2_L-approximation is not valid. They are included just for completeness of the illustration.

IV. CONCLUSION

The self-consistent TFFS [7] is used to calculate the spectroscopic factors of double magic nuclei ^{40}Ca, ^{48}Ca and ^{208}Pb and the chain of semimagic lead isotopes $^{188-212}$Pb as well. In this approach, the SF is related to the Z-factor, the residue of the single-particle Green function in the single-particle pole λ. The self-consistent basis is used of the Fayans EDF [11] with the set of parameters DF3-a [12]. The total Z-factor (18) contains the PC term induced by the low-lying surface excitations, similarly to that considered in Refs. [3, 5, 6]. In addition, it involves the in-volume component due to the energy dependence of the quasiparticle mass operator inherent to the self-consistent TFFS. It is induced by the high-lying in-volume virtual nuclear excitations, the spin-isospin ones playing the main role [14, 15]. The in-volume and PC contributions to the total Z-factor are, as a rule, comparable to each other. The in-volume effect depends weakly on the nucleus under consideration and on the state λ. On the contrary, the PC contribution fluctuates strongly depending on the nucleus and the state λ we deal with.

The experimental SF should be related to the phonon Z-factor $Z^{\rm PC}$ in the case of low-energy reactions with the momentum transfers $q \ll k_{\rm F}$. In the opposite case of $q \gg k_{\rm F}$, the total Z-factor $Z_{\rm tot}$ should be used. In an intermediate situation, the experimental SF should be compared to some intermediate value between $Z^{\rm PC}$ and $Z_{\rm tot}$. Keeping in mind large uncertainties in the absolute values of the "experimental" SFs [18, 19], a direct comparison for each individual case is not much informative. In such a situation, we limit ourselves to the comparison of a tendency in our calculations with the database [17], finding a satisfactory overall agreement.

V. ACKNOWLEDGMENT

The work was partly supported by the Grant NSh-932.2014.2 of the Russian Ministry for Science and Education, and by the RFBR Grants 12-02-00955-a, 13-02-00085-a, 13-02-12106-ofi_m, 14-02-00107-a, 14-02-31353 mol_a.

[1] A. Bohr and B. R. Mottelson, *Nuclear Structure* (Benjamin, New York, Amsterdam, 1969.), Vol. 1.
[2] G. E. Brown, J. A. Evans and D. J. Thouless, Nucl. Phys. **45**, 164 (1963).
[3] V. Bernard and Nguyen van Giai, Nucl. Phys. A **348**, 75 (1980).
[4] A. B. Migdal, *Theory of finite Fermi systems and applications to atomic nuclei* (Nauka, Moscow, 1965; Wiley, New York, 1967).
[5] E. Litvinova, P. Ring, Phys. Rev. C **73**, 044328 (2006).
[6] Li-Gang Cao, G. Colò, H. Sagawa, P. F. Bortignon, arXiv:1401.1983v1.
[7] V. A. Khodel and E. E. Saperstein, Phys. Rep. **92**, 183 (1982).
[8] E. E. Saperstein, S. Kamerdzhiev, S. Krewald, J. Speth and S. V. Tolokonnikov, EPL **103**, 42001 (2013).
[9] N. V. Gnezdilov, I. N. Borzov, E. E. Saperstein and S. V. Tolokonnikov, Phys. Rev. C **89**, 034304 (2014).
[10] E. E. Saperstein, O. I. Achakovskiy, S. Kamerdzhiev, S. Krewald, J. Speth and S. V. Tolokonnikov, Phys. At. Nucl. **77**, 1033 (2014).
[11] S. A. Fayans, S. V. Tolokonnikov, E. L. Trykov, and D. Zawischa, Nucl. Phys. A **676**, 49 (2000).
[12] S. V. Tolokonnikov and E. E. Saperstein, Phys. At. Nucl. **73**, 1684 (2010).
[13] A. B. Migdal, *Theory of finite Fermi systems and applications to atomic nuclei*, 2-nd edition (Nauka, Moscow, 1983).
[14] E. E. Saperstein and S. V. Tolokonnikov, JETP Lett. **68**, 553 (1998).
[15] E. E. Saperstein and S. V. Tolokonnikov, Phys. At. Nucl. **62**, 1302 (1999).
[16] S. V. Tolokonnikov, S. Kamerdzhiev, D. Voytenkov, S. Krewald, and E. E. Saperstein, Phys. Rev. C **84**, 064324 (2011).
[17] http://www.nndc.bnl.gov.
[18] B. K. Jennings, arXiv:1102.3721.
[19] R. J. Furnstahl and H-W. Hammer, Phys. Lett. B **531**, 203 (2002).
[20] E. E. Saperstein and S. V. Tolokonnikov, Phys. At. Nucl. **74**, 1277 (2011).
[21] S. V. Tolokonnikov, S. Kamerdzhiev, S. Krewald, E. E. Saperstein and D. Voytenkov EPJA **48**, 70 (2012).
[22] N. Schwierz, I. Wiedenhöver and A. Volya, arXiv:0709.3525.